Multi-Droplet Evaporative Cooling: Experimental Results

H. F. Dawson and M. di Marzo

Mechanical Eng. Dept., University of Maryland, College Park, MD 20742

Experimental results concerning the evaporative cooling of a Macor tile subjected to a random droplet distribution are reported. The heat input is provided by three radiant panels above the solid surface. The spatial transient temperature distribution over the solid surface and its average surface temperature history are described.

INTRODUCTION

There are a number of engineering and safety applications in which a hot surface is subject to a spray of water droplets. Fire suppression in nuclear powerplants, in process chemical storage, and in fuel storage facilities is a primary application which has inspired a number of experimental and theoretical studies on the phenomena associated with spray cooling. Schoen and Droste [1] investigated the spray cooling of flame engulfed LPG storage tanks to guard against bursting. Davenport [2] also recognized the importance of water spray systems in a study of LPG storage tanks exposed to a fire environment, while Ramskill [3] included spray cooling effects in the computer modeling of exposed tanks. Atallah and Schneider [4] considered the use of water spray curtains as a means of vapor dilution of liquid natural gas in accident situations.

Extensive work has been conducted on the more fundamental aspects of water droplets evaporation. Klassen and diMarzo [5] and Klassen et al. [6] provide a thorough investigation of the evaporation rate of a single droplet gently deposited on low thermal conductivity ceramic surface heated by conduction from below. DiMarzo et al. [7] extended the single droplet experiments to the case of radiant heat input which models more realistically a fire environment. In these studies, the droplet configuration on the solid surface (described by Chandra and Avedisian [8]) is related to the evaporation time, yielding shorter times under conditions of radiant heating.

Research covering the full range of vaporization has been done by Makino and Michiyoshi [9]. DiMarzo and Evans [10,11] formulated the transient conduction problem for an evaporating droplet heated from below by using a simplified, constant and uniform temperature boundary condition at the liquid-solid interface during evaporation. Seki [12] used a similar boundary condition in a study of the transient temperature profile of a hot wall. Numerical integration of the equations in the work by diMarzo and Evans was obtained successfully by diMarzo et al. [13].

The present work constitutes part of a long-term study aimed at modeling the extinguishment of solid fuel fires. In particular, the research presented here investigates the cooling of a radiantly heated solid surface by multiple water droplets evaporation. It is an extension of the previous research efforts given in References [5,6,7]. This study is concerned only with cooling phenomena in a radiant, fire-like environment, where no combustion (hence, no extinguishment) is present. The heated material used is Macor, a glass-like ceramic.

The purposes of this study are: a) to investigate both the temporal and spatial behavior of the surface

temperature of a low thermal conductivity material subject to spray cooling and radiant heat input; b) to continue development of the digital image analysis techniques applied to infrared thermography; c) to gain additional insight into evaporative cooling phenomena, especially for the case of multiple water droplets and d) to obtain data for the validation of a computer code modeling multi-droplet evaporative cooling with radiant heat input.

EXPERIMENTAL APPARATUS

The experimental apparatus is shown in Figure 1. A droplet generator hangs vertically and works in conjunction with a positioning mechanism. Water droplets ejected from the generator impinge upon the Macor tile (square shape with 15.2 cm sides and 2.54 cm thickness) mounted below. The tile rests on a chilled plate to provide a controlled boundary condition at its lower surface. Two radiant panels are positioned on opposite sides of the tile and radiate downward onto the surface at an angle of 30° to the vertical. A third radiant panel surrounds the perimeter of the tile to provide uniform heating to the sides of the Macor. An infrared camera is mounted above and to the side of the tile at an angle of 30° from vertical, and views the surface through a water cooled chilled pipe positioned at the same angle.

The droplet generator produces water droplets with an average volume of 10 ± 1 μl. The primary mechanism for droplet formation is a water filled cavity internal to the generator. A solenoid driven piston produces an indentation in a plastic disk which seals the top of the water filled cavity, thus ejecting a droplet from the generator. The mass flux of the water impinging on the surface is controlled by a time delay relay connected to the solenoid.

A random distribution of water droplets on the surface is achieved by a positioner for the droplet generator. The positioner consists of an aluminum plate with a 25.4 cm hole in the center. Three solenoid driven plastic bumpers are situated around the perimeter of the hole, and simultaneously move radially inward when the solenoids are energized. The droplet generator hangs vertically by four wires in the center of the hole, and motion of the generator is produced when it collides with the moving bumpers. Both the shape of the bumpers and the frequency at which they are activated are optimized to produce a random distribution. The droplets impinge over

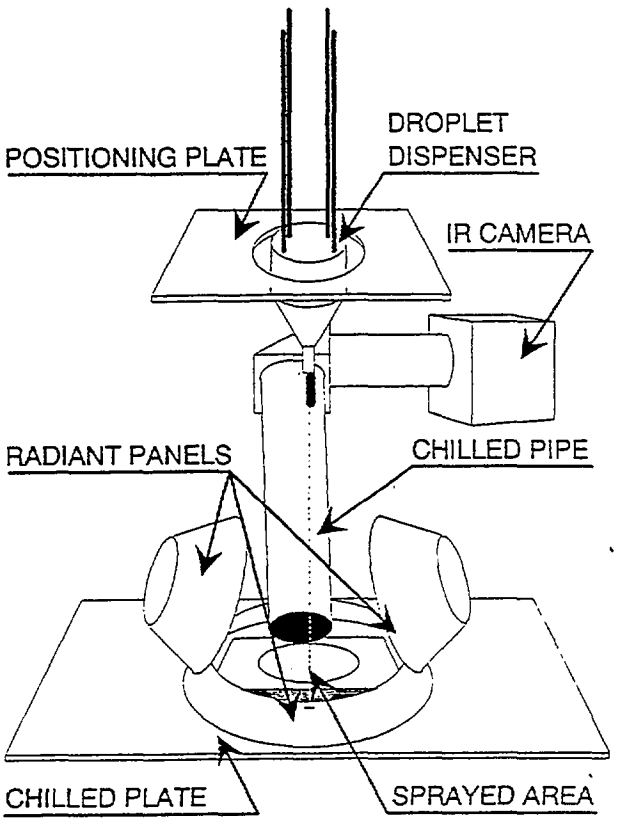

Figure 1. Experimental Apparatus

a circular region with an area of 0.38 cm^2. A typical droplet distribution is shown in Figure 2. This distribution is obtained by marking the landing site of about 200 consecutive droplets delivered by the droplet generator.

The radiant panels used to provide heat input to the surface simulate the heating conditions encountered in an actual fire environment. All three panels are conical in shape and capable of temperatures in excess of 800 °C. Furthermore, they may be approximated to radiate as black-bodies. The panels are connected in a delta circuit and powered by a 208 volt three-phase supply. A temperature feedback loop between the panels and an Omega CN-7100 digital controller maintains the set point temperature of the panels.

An Inframetrics Model 525 infrared camera is the primary data acquisition instrument. The camera uses a 0.61 m focal length closeup lens, and is positioned to view the droplet impingement region of

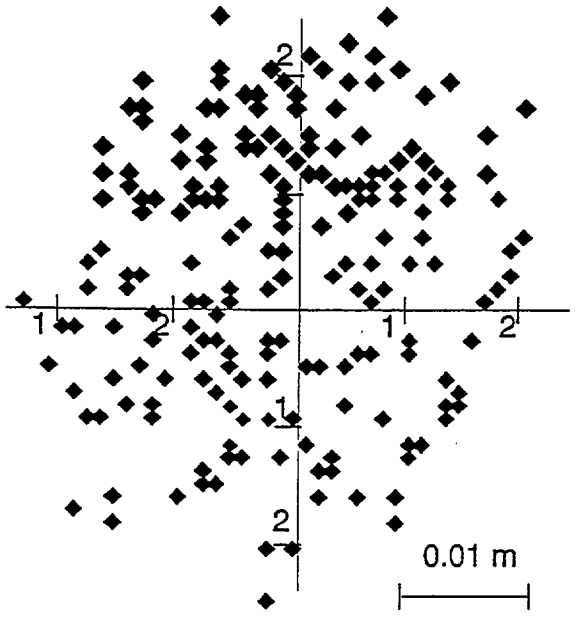

Figure 2. Typical Droplet Distribution

the surface. It produces a real time, monochrome thermal image of the relative temperature distribution on the surface. This image is recorded with a Sony high resolution 8 mm VCR (Hi8) over the duration of an experimental run, producing a complete record of the thermal phenomena occurring on the surface. The geometric orientation of the chilled pipe and the radiant panels is such that reflected radiation from the panels hits the cool, black inner wall of the chilled pipe and is absorbed before reaching the infrared camera. This is important to ensure that only emitted radiation from the surface is recorded as data.

The Macor tile is attached to the chilled plate using Dow Corning silicone heat sink compound. Cold water circulates through the chilled plate, holding the bottom surface temperature of the Macor at a constant value of about 30 °C. This establishes a linear temperature profile between the upper and lower surfaces of the tile, and a uniform temperature on the upper surface before droplets begin to fall.

The relevant properties of Macor are listed in Table 1. Important to note are its relatively high emissivity and low thermal conductivity. Additionally, it has the ability to withstand high thermal stresses, giving a smooth, crack free surface.

Table 1. Macor Properties

Density (kg/m^3)	2520
Thermal Conductivity ($W/m \cdot °C$)	1.297
Specific heat ($J/kg \cdot °C$)	888.9
Emissivity	0.84

EXPERIMENTAL PROCEDURE

The parameters being varied in the experiments are the mass flux of the impinging spray and the initial surface temperature of the solid. In order to ensure consistent thermal conditions, experiments at three different mass fluxes are performed at the same initial temperature in one experimental session. Five initial temperatures of 110 °C, 130 °C, 150 °C, 160 °C, and 180 °C are investigated, while the mass fluxes at each temperature are chosen to preclude the possibility of a surface flooding condition. Over the set of all experiments, these range from .24 $g/m^2 \cdot s$ to 1.6 $g/m^2 \cdot s$. These mass fluxes are nearing the flooding conditions set by the criterion of Grissom and Wierum [14]. It should be noted that the initial temperature of 160 °C corresponds to the onset of nucleate boiling for the Macor surface, while that of 180 °C is in the full nucleate boiling regime. The remaining initial temperatures fall in the evaporative region. The major steps of the experimental procedure are given below.

The water used in the experiments is deionized and degassed. The removal of condensible gasses from the water prior to experiment initiation is essential to obtaining the most controllable experimental conditions. Gasses coming out of solution during the droplet evaporation might alter the configuration of the droplet upon the surface or trigger the onset of nucleate boiling in ways which can be unwieldy to quantify. Water degassing is achieved by consecutive cycles of freezing, vacuum pumping, and thawing. Droplets are tested for bubbles by viewing their evaporation upon a heated surface, and deemed acceptable when no bubbles appear. A sealed water feed to the droplet generator prevents atmospheric gasses from degrading the purity of the final degassed water.

To allow the surface to reach the desired initial temperature, the radiant panels are activated at least two hours prior to experiment initiation. This allows the heater temperature to stabilize to the temperature set on the controller, and most importantly ensures

that the temperature of the solid has reached a steady state condition. The surface temperature is monitored with an Omega thermocouple probe (K-type) read by an Omega digital thermocouple readout. The probe is present on the surface during the heating transient to allow equalization of the probe and surface temperatures.

The infrared camera and all additional electronics (power supply and video components) are also activated two hours prior to experiments to minimize effects of thermal drift. Additionally, water is allowed to begin circulating through the chilled plate and chilled pipe at the time the radiant panels and electronics are turned on. At steady state, before droplets begin to fall, an infrared image of the surface at the initial temperature is recorded. This video image is then digitized using computer resident frame grabbing apparatus (to be described in detail) to assign an actual value to the shades of gray in the image. Ideally, since the surface temperature is uniform, the gray values of the image at each point on the surface are equal, with the exception of random deviations introduced by electronic noise. The average gray value of the surface is then correlated with the initial surface temperature reading to yield a linear relationship of the following form between the temperature at any point on the surface and the gray value at that location. The following expression provides the calibration for a particular initial surface temperature:

$$T = 1.165\ I + T_i \qquad (1)$$

The droplet volume is measured before every run at a given set of conditions. To do this, the droplet generator is turned on and allowed to run for approximately ten minutes to allow the system to stabilize. Fifty droplets are then collected in a beaker of known mass which is quickly capped to avoid evaporation of the droplets. A Metler electronic balance is used to obtain the mass of the water droplets and beaker, ultimately yielding the volume of the droplets. Over the set of all experiments run, droplet volumes range from 8.8 to 11 μl.

Ethyl alcohol is used to clean the surface between each experiment at a different mass flux to remove any impurities or film present. Alcohol sprayed on the surface is allowed to evaporate, and the surface is then rinsed with distilled water. This is repeated and the surface is then given time to return to the initial temperature.

For each experiment conducted at a particular set of conditions, droplets impinge upon the heated surface for a period of twenty five minutes while the infrared image is recorded onto videotape. During this time, the image being recorded can be viewed on a video monitor. For a few seconds before each recorded run on the videotape, a regular TV camera is used to record a portion of a blackboard containing pertinent information about the run (droplet volume, initial surface temperature, mass flux, heater temperature, ambient temperature, and chilled plate temperature). The information contained on the videotape is then sufficient to determine both transient and spatial temperature information about the surface in the experimental data processing and reduction.

DATA PROCESSING AND REDUCTION

At the completion of one set of experiments at a given initial temperature, data processing is performed. Two types of information can be obtained from the video record: a) the transient behavior of the average surface temperature and b) the spatial temperature distribution on the surface at any time into the transient. Common to both analyses is the video digitization system used to extract gray values from the recorded image. A Matrox MVP-AT frame grabber is used to digitize individual frames, of duration 1/30 of a second, into a discrete number of gray shades. Subroutine libraries included with the frame grabber (Imager-AT software) are linked with user written source code to access the gray value of each pixel of the digitized image individually. This value is then correlated with a temperature to perform the desired analysis. The specific method of analysis for each case is now discussed.

The transient behavior of the average surface temperature is obtained by digitizing individual frames of the recorded surface at intervals of 30 seconds starting at the beginning of the run. A computer program is used to average the gray values of every fifth pixel in the image, corresponding to 3717 pixels over a 5 cm x 5 cm region of the surface. An average pixel value for the surface at that particular time during the transient is thus obtained, which is then used with Equation (1) to determine the average surface temperature.

The resulting data are fit to a decaying exponential curve of the following form:

$$T = (T_i - T_{ss})\, e^{-t/\tau} + T_{ss} \qquad (2)$$

where τ is the time constant of the fit and T_{ss} the steady state temperature. Both of these parameters are adjusted to obtain the best fit. A total of 130 gray shades are used to resolve an average temperature range of 100 °C, resulting in a thermal resolution of 0.76 °C/gray shade.

To obtain the spatial distribution of the temperature at a specific time into the transient, each pixel in a digitized frame is accessed individually. From knowledge of the area of the viewed region and the pixel location in the image, an cartesian coordinate is determined along with the gray shade for each pixel. The temperature at a particular location is then determined from Equation (1). This is done for the same number of pixels as in the transient analysis, and the results plotted as a three dimensional surface of the temperature versus the cartesian coordinates (i.e. x and y). The spatial resolution achieved using these techniques is 0.14 mm/pixel, corresponding to a 512 (horizontal) x 480 (vertical) pixel image of a viewed region 7.2 cm x 6.7 cm. Note that the area of the viewed region is somewhat smaller than the wetted area. This is necessary to achieve the best focus with the infrared camera.

RESULTS AND DISCUSSION

Three dimensional plots of the temperature distribution on the Macor surface are shown in Figures 3(a-c), 4(a-c), and 5(a-c) for the indicated initial temperatures and mass fluxes. The results are especially notable in that they represent a detailed description of the temperature at any point on the surface, obtained with highly non-intrusive techniques. Each sequence of plots shows the surface temperature distribution at three different times; 1) early in the transient, 2) further on in the transient, and 3) at or approaching steady state. The most distinct features are the large dips in the temperature, especially at times early in the transient. These are regions where individual droplets have landed, and caused a rapid local cooling effect. The average surface temperature is seen to be still very near the initial value. At later times, the average surface temperature begins to drop

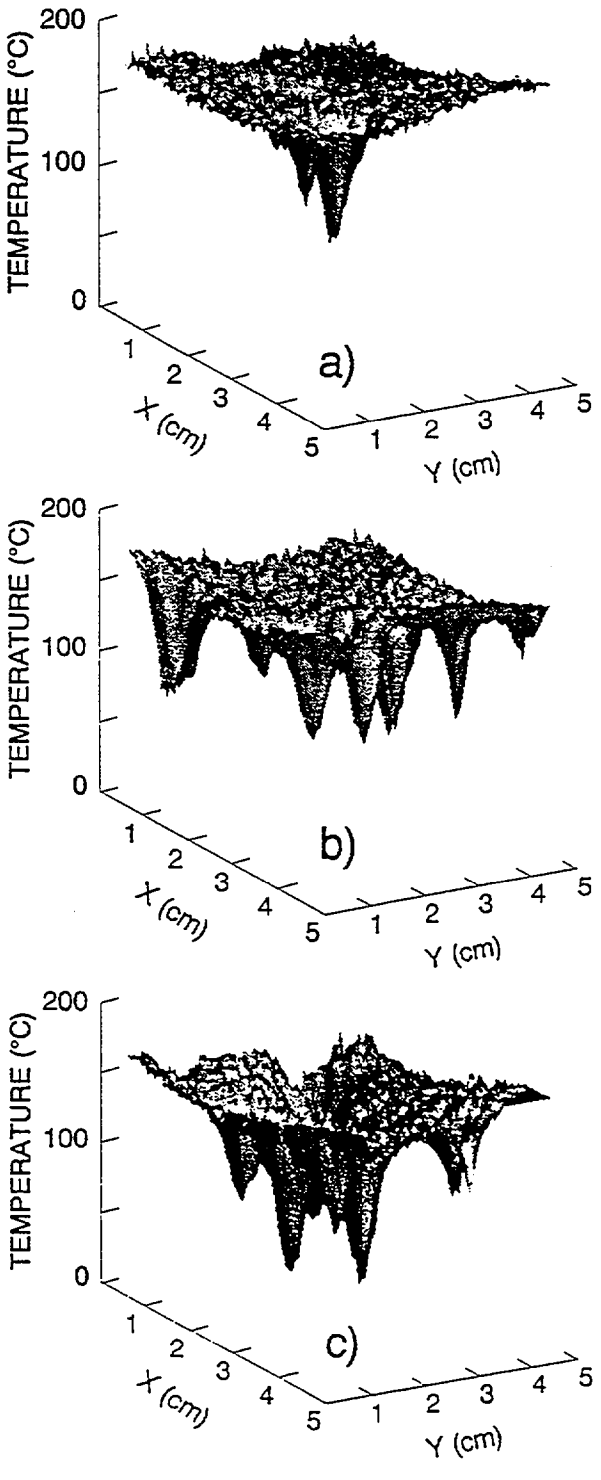

Figure 3. Solid Surface Temperature Distribution for T_i = 182 °C and G = 0.86 g/m²s (a: t = 5s; b: = 240s; c: = 600s)

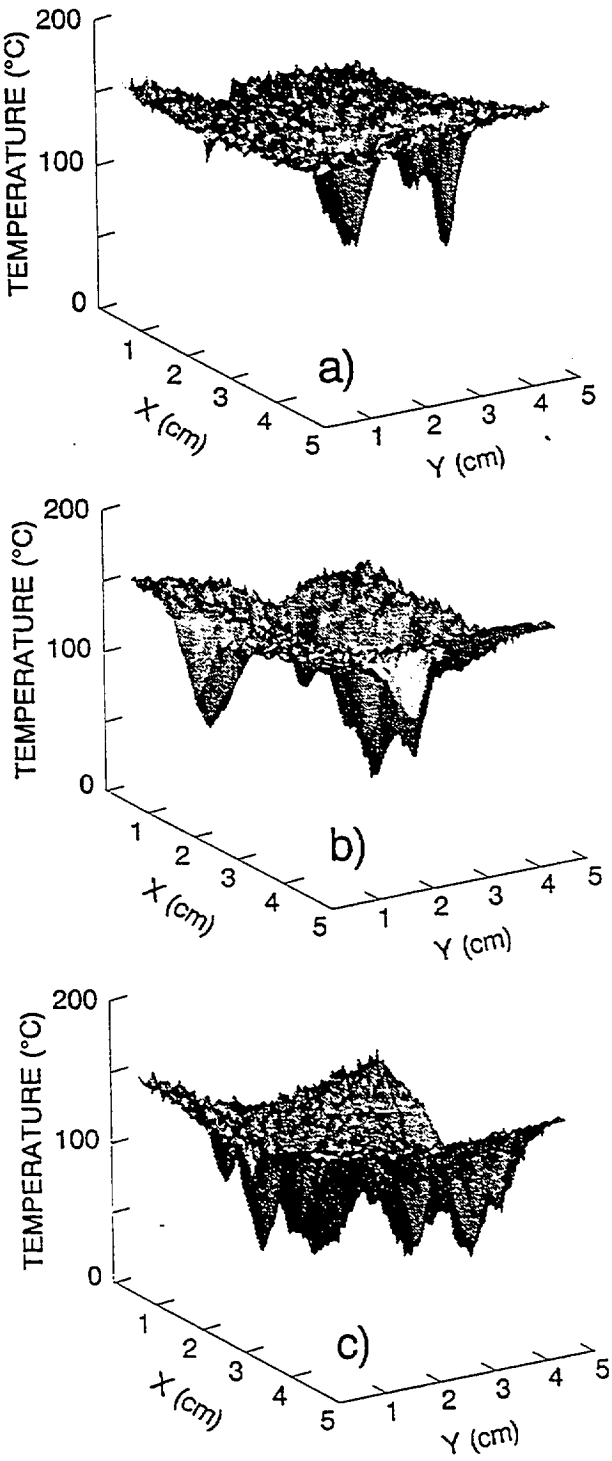

Figure 4. Solid Surface Temperature Distribution for T_i = 162 °C and G = 0.97 g/m^{2}s (a: t = 5s; b: = 240s; c: = 600s)

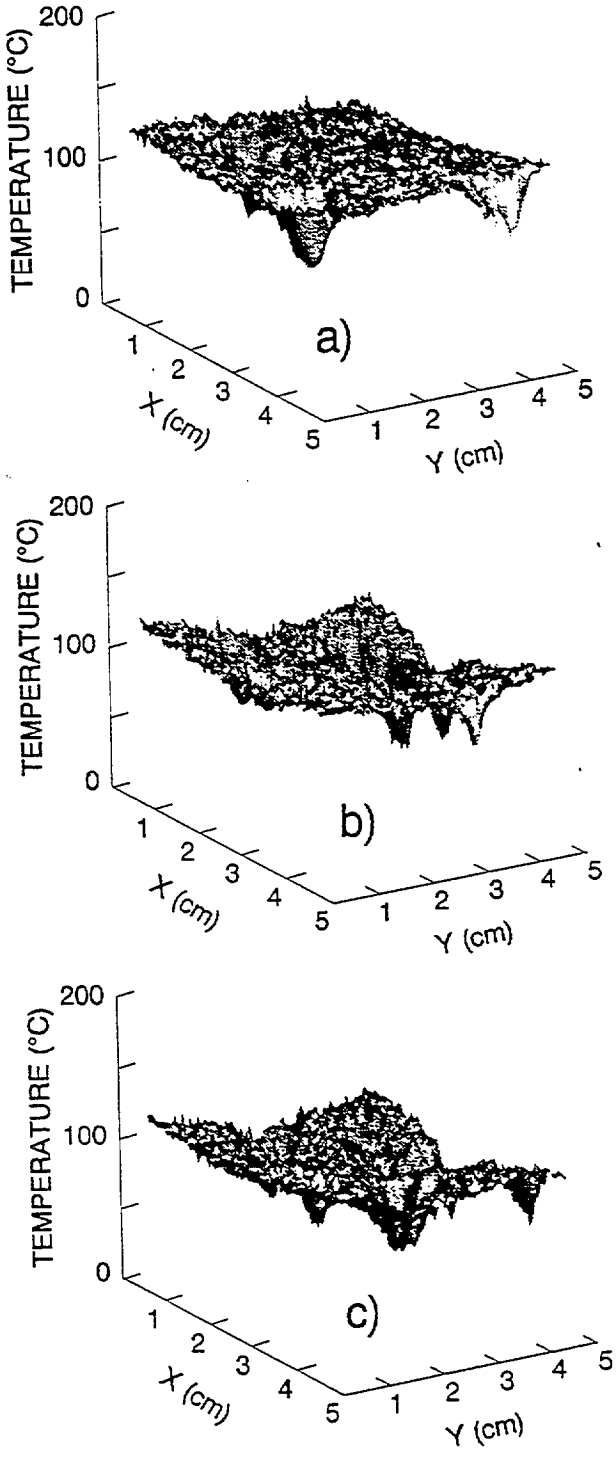

Figure 5. Solid Surface Temperature Distribution for T_i = 131 °C and G = 0.50 g/m^{2}s (a: t = 5s; b: = 240s; c: = 600s)

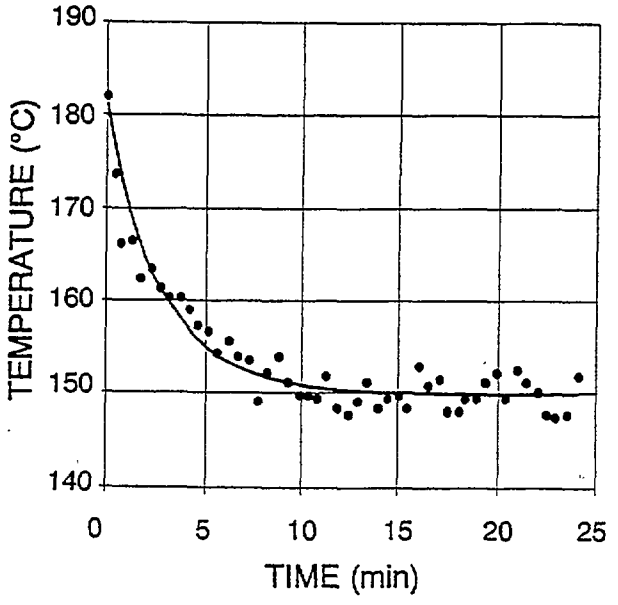

Figure 6. Transient Average Surface Temperature for T_i = 182 °C and G = 0.86 g/m^{2}s

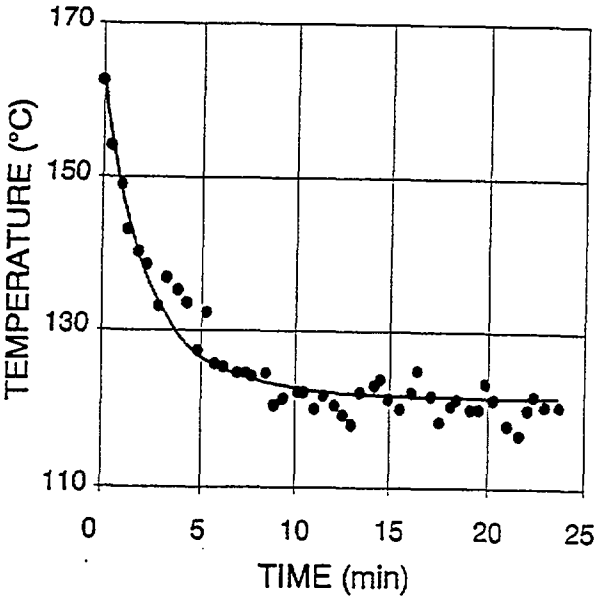

Figure 7. Transient Average Surface Temperature for T_i = 162 °C and G = 0.97 g/m^{2}s

from the initial value, since the droplets have cooled the surface sufficiently such that the effects of individual droplets tend to superimpose with one another for more uniform cooling. As the surface temperature approaches a steady state, the individual droplets become more difficult to discern and the plot surface more wave-like. An error of ± 2 °C is evident from the plots, and results primarily from variations in pixel intensity caused by surface irregularities and electronic noise.

Graphical results of the average surface temperature versus time are shown in Figures 6, 7, and 8. The raw data are shown along with the best fit exponential decay for each case. The initial temperatures shown include both convective and nucleate boiling. Examination of the plots reveals important features which can be seen in all the cases. The most significant is the clear decay to a steady state temperature. In all cases a steady state condition is reached at a time no later than ten minutes after initial droplet deposition. A comment on the oscillatory nature of the average surface temperature is necessary. Such behavior arises because only a portion of the actual sprayed area is viewed by the infrared camera. Therefore, at any time, there may be a different number of droplets

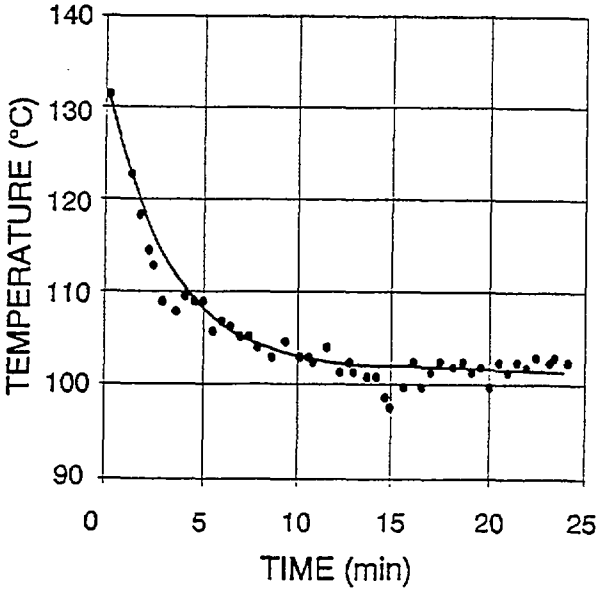

Figure 8. Transient Average Surface Temperature for T_i = 131 °C and G = 0.50 g/m^{2}s

on the surface than at other times, resulting in overall pixel intensity variations in the image.

An energy balance is performed on the hot surface to provide verification of the results by calculating a steady state temperature. Equating the heat input from the radiant panels to the heat released from the Macor by radiative exchange, convection, and conduction yields the following balance of terms:

$$\epsilon \sigma F T_h^4 = h(T_i - T_\infty) + \frac{k}{d}(T_i - T_b) \quad (3)$$

Note that the net conductance h embodies both convective and radiative mechanisms. Additionally, Kirchoff's Law for a gray surface has been used. At steady state the same energy balance is written as:

$$\epsilon \sigma F T_h^4 - \lambda G = h(T_{ss} - T_\infty) + \frac{k}{d}(T_{ss} - T_b) \quad (4)$$

By subtracting Equation (4) from Equation (3), one obtains:

$$\lambda G = h(T_i - T_{ss}) + \frac{k}{d}(T_i - T_{ss}) \quad (5)$$

Rearrangement provides an analytical expression for the steady state temperature:

$$T_{ss} = T_i - \frac{\lambda G}{h + \frac{k}{d}} \quad (6)$$

With h calculated from Equation (3) and used in Equation (6), the measured steady state temperature versus the calculated value is shown in Figure 9. Agreement of the best fit straight line is best at higher temperatures and deviates slightly at lower values. A likely explanation is that the view factor between the heaters and the surface, F = 0.26 (obtained by measuring the incident radiation), is slightly in error, which can have a significant effect on h and thus T_{ss}. Another possible source of error is that the temperature underneath individual droplets

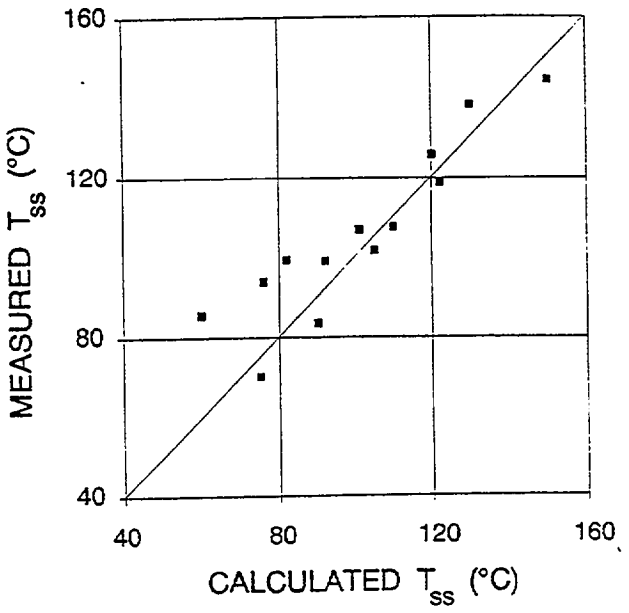

Figure 9. Experimental and Calculated Steady State Temperature

is under-estimated. This would occur because the calibration used to obtain the temperatures is only valid for the Macor surface. When the camera records a water droplet that has not yet evaporated, the calibration no longer applies since a water droplet and not the surface is being viewed. Approximately 10% of the surface is covered at a given time. This percentage of the average temperature drop underneath a droplet, approximately 40 °C, gives an estimate of 4 °C by which the average temperature is in error.

The best fit curve to the transient data is determined by inspection of the data to ascertain the steady state temperature used in the fit. The time constant τ is then adjusted to introduce the least spread in the points around the curve. It might be expected that at higher mass fluxes, τ would be smaller due to the increased cooling capacity of the higher flux spray. Accordingly, the time constants (deduced from the best fit of the data) from each experiment are plotted versus the mass flux in Figure 10. From the figure, no apparent relationship is evident, suggesting that the properties of the Macor may be the more dominant factors influencing the time scale of the phenomenon. Pursuing this idea, a general expression for the penetration depth in the

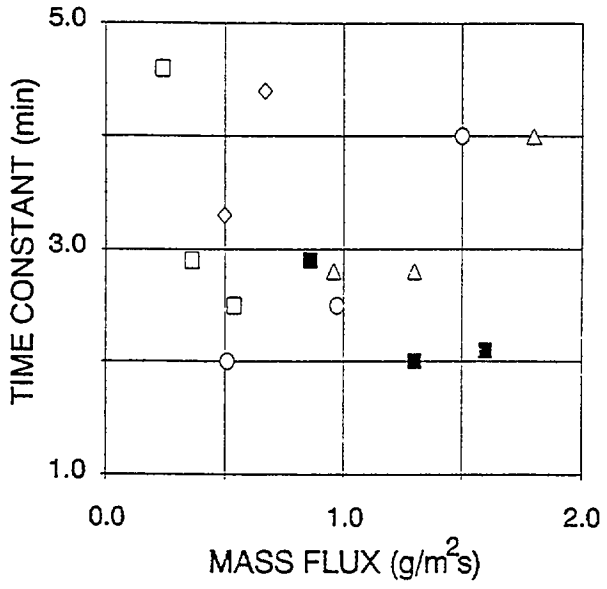

Figure 10. Transient Time Constant for Various Water Mass Fluxes and Initial solid Surface Temperatures (■: T_i = 182 °C; ○: T_i = 162 °C; △: T_i = 151 °C; ◇: T_i = 131 °C; □: T_i = 111 °C)

solid is given by:

$$\delta = \sqrt{\alpha \tau} \qquad (7)$$

Substituting 5.8 x 10^{-7} m^2/s for the thermal diffusivity of Macor, and an average τ of 170 seconds from Figure 10 yields δ = 1 cm. This can be compared to the radius of influence of a single droplet, as discussed by Klassen and diMarzo [5]. Essentially, it is a measure of the cooling effect a single droplet has upon the region surrounding it. On Macor, this corresponds to a circular region four times the radius of a droplet on the surface, or 0.5 cm. This is on the same order as δ, and suggests that the time constant is more closely linked to thermophysical properties of the material than to the impinging mass flux.

CONCLUSIONS

The spatial and temporal behavior of the temperature of a radiantly heated, low thermal conductivity surface cooled by multiple water droplets evaporation was experimentally investigated over a range of different initial surface temperatures and mass fluxes. For all conditions, the average surface temperature decreases exponentially with time before reaching a steady state value. The measured steady state temperature agrees well with that calculated from an energy balance, with the best agreement achieved by considering small variations in the view factor between the heaters and surface. Slight variations in the view factor, due to small inaccuracies in spatial measurements used to determine it, can result in over-estimation of the overall heat transfer coefficient, resulting in lowered calculated temperatures.

The spatial distribution of the surface temperature shows a decrease in the average temperature, as suggested by the transient results, and provides a thorough description of the temperature at a point on the surface at any time. There appears to be no strong correlation between the impinging mass flux and the time constant of the exponential temperature decay. A length scale determined using properties of the solid material suggests that the characteristic time scale of the phenomenon is more likely a function of these properties.

The data acquisition system used, employing digital image analysis and infrared thermography, provides a high degree of thermal and spatial resolution. Additionally, it represents a novel approach to non-intrusive temperature measurement for this type of application.

ACKNOWLEDGEMENTS

This research has been sponsored by a grant of the Building and Fire Research Laboratory of the National Institute of Standards and Technology.

NOTATION

d	thickness of Macor tile
F	view factor between radiant panels and surface
G	water mass flux
I	average gray value
h	overall heat transfer coefficient
k	thermal conductivity of Macor
T	temperature
T_b	Macor bottom surface temperature
T_i	initial solid surface temperature
T_h	radiant panel temperature

T_{ss} steady state surface temperature
T_∞ ambient temperature
t time

α thermal diffusivity of Macor
δ penetration depth
ϵ emissivity of Macor
λ water latent heat of vaporization
σ Stefan-Boltzman constant
τ time constant

LITERATURE CITED

1. Schoen, W. and B. Droste, "Investigation of Water Spraying Systems for LPG Storage Tanks by Full Scale Fire Tests," *Journal of Hazardous Materials*, 20, 73-82, (1988).

2. Davenport, J., "Hazards and Protection of Pressure Storage and Transport of LP-GAS," *Journal of Hazardous Materials*, 20, 3-19, (1988).

3. Ramskill P.K., "A Description of the "ENGULF" Computer Codes - Codes to Model the Thermal Response of an LPG Tank Either Fully or Partially Engulfed by Fire," *Journal of Hazardous Materials*, 20, 177-196, (1988).

4. Atallah, S., and A.L. Schneider, "LNG Safety Research in the USA," *Journal of Hazardous Materials*, 8, 25-42, (1988).

5. Klassen, M. and M. diMarzo, "Transient Cooling of a Hot Surface by Droplet Evaporation," *National Institute of Standard and Technology Report*, NIST-GCR-90-575, (1990).

6. Klassen, M., M diMarzo and J. Sirkis, "Infrared Thermography of Dropwise Evaporative Cooling," *ASME-HTD*, 141, 117-121, (1990).

7. diMarzo, M., C.H. Kidder, and P. Tartarini, "Infrared Thermography of Dropwise Evaporative Cooling of A Semi-Infinite Solid Subjected to Radiant Heat Input," *Experimental Heat Transfer*, 5, 101-104, (1992).

8. Chandra, S. and C.T. Avedisian, "On the Collision of a Droplet with a Solid Surface," *Proceedings of the Royal Society of London*, 432, 13-41, (1991).

9. Makino, K. and I. Michiyoshi, "The Behavior of a Water Droplet on Heated Surfaces," *International Journal of Heat and Mass Transfer*, 27, 781-791, (1984).

10. diMarzo, M. and D.D. Evans, "Dropwise Evaporative Cooling of High Thermal Conductivity Materials," *Heat and Technology*, 5, (1-2), 126-136, (1989).

11. diMarzo, M. and D.D. Evans, "Evaporation of a Water Droplet Deposited on a Hot High Thermal Conductivity Solid Surface," *Journal of Heat Transfer*, 111, 210-213, (1989).

12. Seki, M., H. Kawamura and K. Sanokowa, "Transient Temperature Profile of a Hot Wall Due to an Impinging Liquid Droplet," *Journal of Heat Transfer*, 100, 167-169, (1978).

13. diMarzo, M., P. Tartarini, Y. Liao, D.D. Evans and H. Baum, "Dropwise Evaporative Cooling," *ASME-HTD*, 166, 51-58, (1991).

14. Grissom, W.M. and F.A. Wierum, "Liquid Spray Cooling of a Heated Surface," *International Journal of Heat and Mass Transfer*, 24, 261-271, (1981)